minerals

IMPACT FACTOR 2.5

CITESCORE 3.9

Article

Adding Value to Mine Waste through Recovery Au, Sb, and As: The Case of Auriferous Tailings in the Iron Quadrangle, Brazil

Mariana Gazire Lemos, Teresa Maria Valente, Amélia Paula Marinho Reis, Rita Maria Ferreira Fonseca, Fernanda Guabiroba, José Gregorio da Mata Filho, Marcus Felix Magalhães, Itamar Daniel Delbem and Giovana Rebelo Diório

Special Issue

Metallurgical Solid Waste: Mineralogy, Chemistry and Application/Treatment

Edited by

Dr. Wentao Hu and Dr. Hong Peng

MDPI

https://doi.org/10.3390/min13070863

minerals

MDPI

Article

Adding Value to Mine Waste through Recovery Au, Sb, and As: The Case of Auriferous Tailings in the Iron Quadrangle, Brazil

Mariana Gazire Lemos [1,2,*], Teresa Maria Valente [1], Amélia Paula Marinho Reis [1], Rita Maria Ferreira Fonseca [3], Fernanda Guabiroba [2], José Gregorio da Mata Filho [2], Marcus Felix Magalhães [2], Itamar Daniel Delbem [4] and Giovana Rebelo Diório [5]

[1] Institute of Earth Sciences, Pole of University of Minho, Universidade do Minho, Campus de Gualtar, 4710-057 Braga, Portugal; teresav@dct.uminho.pt (T.M.V.); pmarinho@dct.uminho.pt (A.P.M.R.)
[2] Anglogold Ashanti, Mining & Technical, COO International, Nova Lima 34000-000, Brazil
[3] Institute of Earth Sciences, Pole of University of Évora, University of Évora, 7000-345 Évora, Portugal; rfonseca@uevora.pt
[4] Microscopy Center, Universidade Federal de Minas Gerais, Belo Horizonte 31270-013, Brazil; danieldelbem@gmail.com
[5] Laboratory on Basin Analysis, Universidade Federal do Paraná, Curitiba 81532-980, Brazil; g.rebelo.d@gmail.com
* Correspondence: id8548@alunos.uminho.pt

Abstract: From the colonial era to modern times, gold mining has played a crucial role in shaping Brazil's economy, culture, and landscape, particularly in the Iron Quadrangle region. Therefore, resulting waste has accumulated in tailings structures, either from deactivated circuits or plants still in production. The present study reveals the potential assessed based on a set of metallurgical tests, assuming specific scenarios depending on the occurrence modes of interesting economic elements. For Au, calcination, leaching, and flotation are promising techniques to recover this element. Tests indicated that toxic elements such as Sb and As could be effectively reused in the form of glass. The generation of other products from dry cleaning techniques was not effective but promising since there was an enrichment of elements with Au, Fe, Al, and K in specific fractions.

Keywords: tailings properties; circular economy; metallurgical tests; Au recovery; As recovery; Sb recovery

Citation: Lemos, M.G.; Valente, T.M.; Marinho Reis, A.P.; Ferreira Fonseca, R.M.; Guabiroba, F.; da Mata Filho, J.G.; Magalhães, M.F.; Delbem, I.D.; Rebelo Diório, G. Adding Value to Mine Waste through Recovery Au, Sb, and As: The Case of Auriferous Tailings in the Iron Quadrangle, Brazil. *Minerals* **2023**, *13*, 863. https://doi.org/10.3390/min13070863

Academic Editor: Wentao Hu

Received: 23 May 2023
Revised: 19 June 2023
Accepted: 23 June 2023
Published: 26 June 2023

1. Introduction

Socio-political changes and population growth are crucial factors for the exploration of new mineral assets [1,2]. The United Nations (UN) projects a continuous increase in global population, reaching 9 billion by 2030 and 10 billion by 2050, with a corresponding rise in urban areas [3]. Urbanization and population density are strongly linked to the consumption of metals and minerals, and this sector influences others by supplying raw materials to several industries [4]. As a result, the mineral industry has become the world's largest waste producer, generating ca. 65 billion tons/year, of which 14 billion consist mostly of fine (<150 µm) particles [5].

An important noble metal is gold (Au), widely used in jewelry manufacturing and as a monetary reserve. South Africa holds 40% of the world's gold reserves, while Brazil contributes approximately 2% [6,7]. Brazil's minable Au reserves amount to nearly two thousand tons. During the extraction and processing of gold-bearing rocks, various processes such as crushing, grinding, gravimetry, flotation, and cyanidation are employed [6]. However, due to the low ore concentration in host rocks, mining operations generate significant amounts of tailings [8]. In Brazil, the Au mining industry produces approximately 600 million tons of tailings annually, and this figure is projected to reach almost 1 billion tons by 2030 [9].

There are other problems associated with current mining methods. Metals are often linked to contamination, which poses risks to ecosystems and human health. It is crucial to understand toxicities, percolation processes, and human absorption mechanisms to enhance research on their environmental impacts and ecological risks [10]. For instance, elements like arsenic (As) and metals such as zinc (Zn), lead (Pb), nickel (Ni), and antimony (Sb) are commonly found in association with Au waste, presenting a high potential for contamination [11–14]. Moreover, the geopolitical context and the monopoly of strategic commodities in specific countries, along with events such as Russia–Ukraine conflict and the COVID-19 pandemic, directly affect raw materials supply chains. Recent assessments have identified 87 individual raw materials, most found in mining waste, as critical due to these factors [15,16]. Finally, environmental disasters related to waste and tailing, including recent ones in Brazil, further highlight the significance of these issues [13].

With market and technological advances, tailings can serve as an alternative to primary exploitation. Thus, in line with sustainable development objectives and other circular economy goals, it is crucial to investigate the reuse of mining tailing worldwide [6,16]. This can be achieved through the application of innovative new technologies to extract value from low-grade "ores" or by repurposing tailings for various uses [1,12,17–19]. However, each situation is unique, and ongoing research and analysis are necessary to explore these opportunities further.

The potential for Au recovery from various types of tailings has been extensively investigated. Flotation and cyanidation tests are the primary methods employed to reprocess such material, sometimes involving additional stages such as regrinding, roasting, and cyanidation of flotation concentrates. In certain studies [20], Au dissolution and recovery rates ranged from 87.8% to 98.4% in sulfide-containing Au tailings. Advances in processing technology, coupled with the residual Au content found in aged cyanidation tailings, offer opportunities for developing recovery routes for Au present in these wastes [21]. Reprocessing gold mine tailings has proven to be economically viable and beneficial, particularly when integrated into existing facilities to compensate for raw ore shortages and operational losses [22]. Some plants currently incorporate Au tailings reprocessing into their production chains, such as the Elikhulu tailings re-treatment plant (Southern Africa), which processes 1.2 Mt of historic tailings per year from three existing slime dams [23] and Paracatu mine (Brazil) in which 10 million tons of hydrometallurgy tailings containing 1 mg Au/kg are reprocessed [24]. Furthermore, health-hazard elements, which occur alongside Au, can also possess industrial value [11–14]. Moreover, state-of-the-art research indicates that gangue minerals found in tailings have significant potential for application in civil construction and even as fertilizers, depending on properties such as granulometry and chemical composition [25–29].

Hence, the vast volumes of waste generated by mining and mineral processing, combined with geopolitical contexts, significant environmental impacts, and risks to human health, justify the importance of adding value to tailings. In light of these challenges, this study was conducted in the region of Santa Barbara and Nova Lima cities (Brazil), encompassing four active and inactive Au tailings dams, as well as three piles and tailings from depleted mines. The objective of this article is to evaluate the potential for value addition to the waste in this area and explore options for its reuse, not solely limited to the recovery of valuable elements such as Au, Sb, and As. For recoveries of these elements, this paper will go through steps of characterization, extraction of elements by flotation, leaching, calcination, and even the use of vitrification techniques. In addition, a study attempting to reuse other elements was performed using dry concentration (recovery using triboelectrostatic stages). The applications of the generated products can be directly used in the metallurgical industries, such as the production of gold bars, in the textile industry, in the production of plastics, and in sectors such as fertilizers and building materials. In addition, reuse can be an important tool for the resolution of environmental liabilities and pollution control, such as the neutralization of toxic elements like As.

2. Study Area

The seven tailing structures investigated in this study are located in the main Brazilian mineral province known as Iron Quadrangle (IQ; Figure 1). Among these structures, five are situated in Nova Lima, while the remaining two are found in Santa Barbara, in Minas Gerais, Brazil. Both cities have a long-standing history of Au mining, dating back to the 19th century, and continue to be significant Au production regions in Brazil. These metallogenic Au deposits are hosted within the Rio das Velhas Greenstone Belt, which is recognized as the biggest Au district in Brazil [30,31].

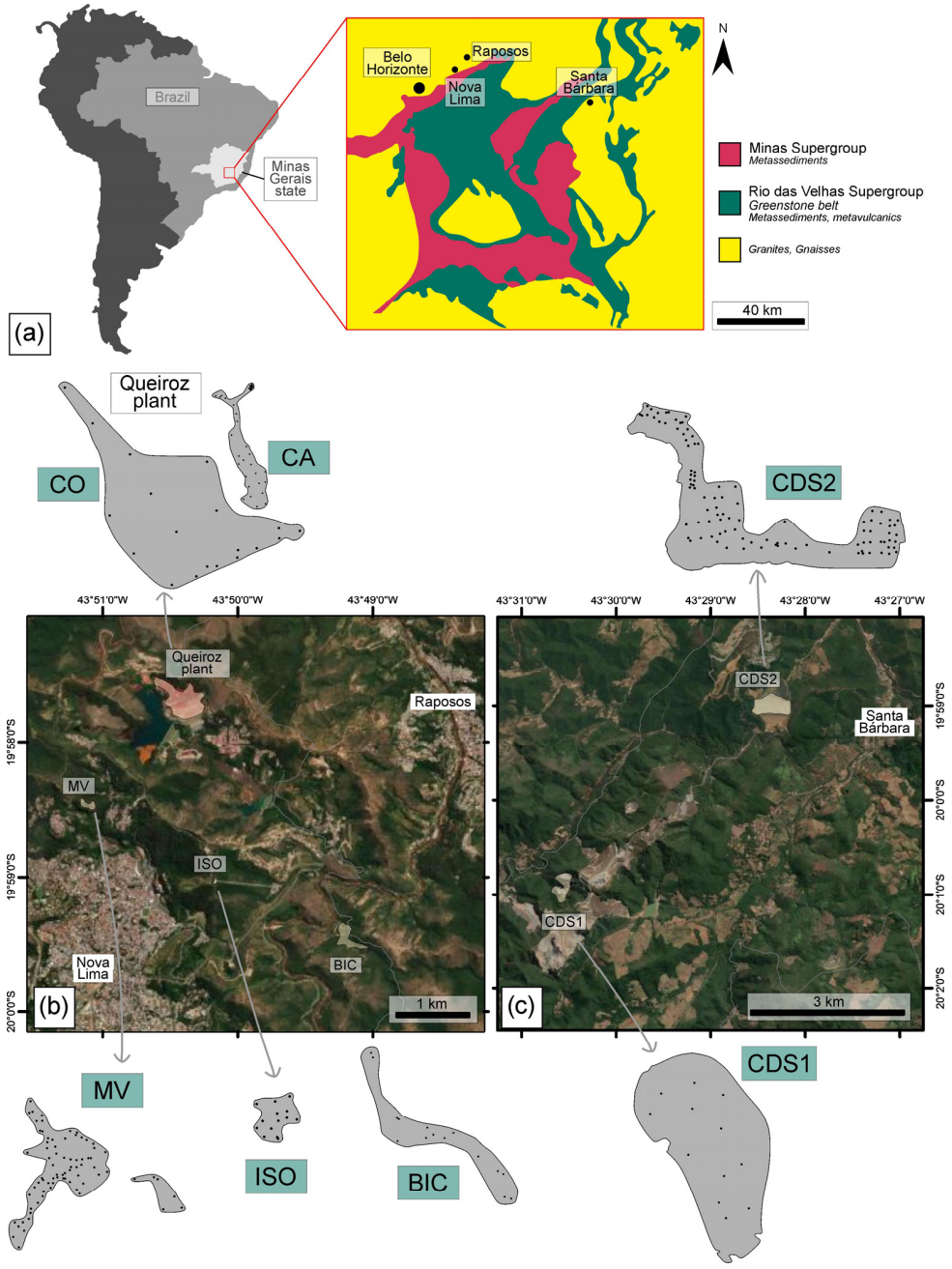

Figure 1. (**a**) Location of the studied sites within the IQ, as shown in the modified schematic map from [32]. Dams and tailing piles in (**b**) Nova Lima (MV, ISO, and BIC) and (**c**) Santa Barbara (CDS1, CDS2), along with the sampling locations (black dots).

Santa Bárbara dam and tailing piles are situated in the northern part of the IQ, in Santa Bárbara city, ca. 110 km away from Belo Horizonte, the capital of Minas Gerais state.

These waste deposits have been accumulating since 1986, receiving the tailings generated from Au underground mines and processed at metallurgical plants. The tailings at this site originated from different sources and exhibited distinct characteristics: (a) oxidized tailing piles resulting from the heap leach plant that receives ore extracted from open pit mines (CDS1; Figure 2a); and (b) tailing dams from flotation and leaching plant, fed by fresh ores from underground mining operations (CDS2; Figure 2b).

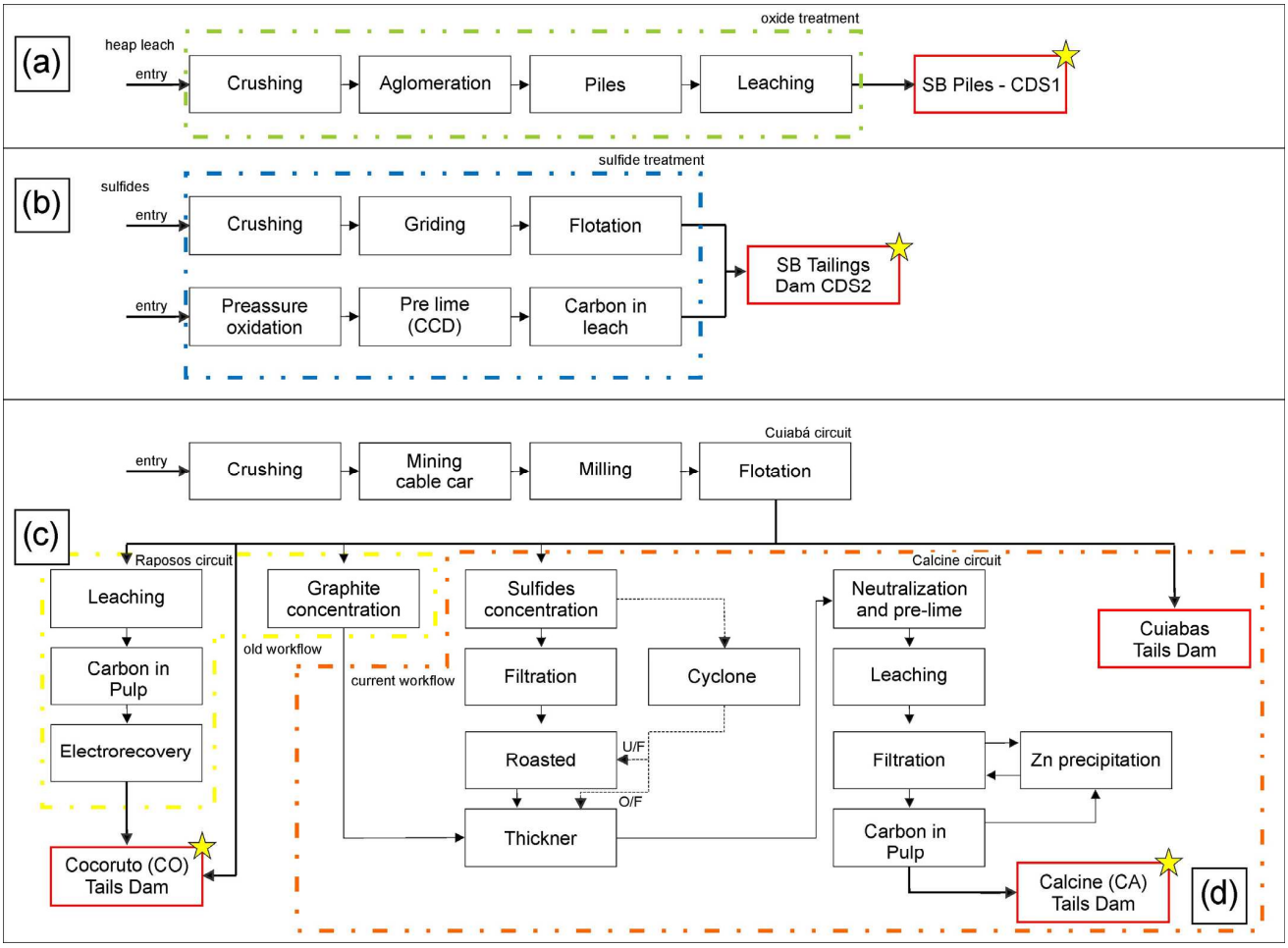

Figure 2. Waste generation flowchart for (**a**) CDS1, (**b**) CDS2, and Queiroz plant—(**c**) CO (Cocoruto) and (**d**) CA (Calcine) samples. Sample locations are marked with a yellow star. Modified from [33,34].

The Nova Lima mines encompass both inactive and active operations, with a significant presence of tailings from deposits that have been exploited since the previous century. Waste from local mines has been accumulating since 1834, and the estimated Au reserves in the area currently amount to ca. 107 tons [35]. The main structures are the (1) Isolamento tailings deposit (ISO); (2) Bicalho inactive mine dam (BIC); (3) deposits at the Mina Velha (MV) plant; and (4) active and inactive dams at Queiroz metallurgical plant (CA and CO) (Figure 2).

These dams and tailing deposits are in the northern part of the IQ, from near the cities of Nova Lima and Raposos, ca. 25 km away from Belo Horizonte (Figure 1). Within ISO, BIC, and MV, a wide variety of waste materials from historical Au plants have been deposited. The presence of waste from the previous century suggests that these tailings may originate from Au extraction processes that predate the use of cyanide. Unfortunately, due to the lack of historical archives, accurately describing the extraction processes becomes challenging; however, it is believed that wastes predominantly result from gravimetric processes [35].

In contrast, the Queiroz plant has been processing Fe sulfide with Au ores for over thirty years. The materials treated at the factory are divided into two distinct circuits. The Raposos circuit (Figure 2c) primarily treats non-refractory sulfide ore from Raposos mines. This circuit achieves an Au recovery rate of 90% through various treatment stages, including milling, gravity separation, conventional leaching, CIP (carbon leaching) process, elution, and electro-recovery. The resulting tailings from this circuit are deposited in the Cocoruto (CO) tailings basin. However, the Raposos circuit and the associated metallurgical process stage were deactivated in 1998, along with the Raposos mine [13,33,35]. Currently, the Queiroz plant circuit treats refractory Au, which requires an additional calcination step after milling and flotation (Figure 2d). Following calcination, Au is recovered through leaching, CIP (leaching carbon), elution, and electro-recovery [13,33,35,36]. The resulting tailings are then deposited in the calcined dam (CA).

3. Methodology

3.1. Characterization of Tailing Samples

3.1.1. Sampling

The sampling stage was conducted during late winter and early spring in south-eastern Brazil (Figure 1). Samples were obtained through drilling at varying depths, depending on the specific structure being assessed. Subsequently, individual samples were combined to create composite samples, which represented each tailings structure for the recovery/reuse tests.

3.1.2. Sample Composition

Multielement analysis to assess the reuse of the composite samples and metallurgical test products was conducted using inductively coupled plasma mass spectrometry (ICP-MS, PerkinElmer SCIEX, Waltham, MA, USA). Prior to analysis, acid digestion (nitric acid, hydrogen peroxide, and hydrochloric acid) was performed at the laboratory of AngloGold Ashanti and SGS Geosol in Brazil. Sulfur (S) and carbon (C) concentrations were evaluated using infrared (IR) analysis (LECO, St Joseph, MI, USA, with a detection limit of 0.01%). Au analysis was carried out using atomic absorption spectroscopy with the fire test method (AAS, Varian, Palo Alto, CA, USA, with a detection limit of 0.05 mg/kg). To ensure the quality and accuracy of the analyses, duplicates, blanks, and standard reference materials (Si81 from Rocklabs) were included.

3.1.3. Particle Size Distribution

The particle size distribution (PSD) was obtained using the MasterSizer 3000 equipment (Malvern Instruments Ltd., Worcestershire, UK). Laser diffraction was employed for this analysis, and composite samples were used. The PSD results were categorized as follows: <2 μm for mud fraction, 2–20 μm for fine silt, 20–63 μm for coarse silt, and 63–2000 μm for the sand fraction.

3.1.4. Mineralogy

Composite samples were submitted to a mineralogical study employing various techniques, including optical microscopy, X-ray diffraction (XRD), and scanning electron microscopy (SEM—Field Electron and Ion Company—FEI), conducted at the Universidade Federal de Minas Gerais (Belo Horizonte, Brazil) and University of Minho (Braga, Portugal).

The mineralogical composition was determined using XRD analysis with an X'pert Pro-MPD diffractometer (Philips PW 1710, APD), using CuKα radiation, and equipped with an automatic divergence slit and graphite monochromator. The diffractograms were obtained from <2 mm powders fraction, covering a range of 3 to 65° 2θ with a 2θ step size of 0.02° and a counting time of 1.25 s [36]. In addition, fifty thin polished sections by structure were analyzed using a Leica optical microscope and a FEI electron microscope, Quanta 600 FEG, high vacuum mode, coupled to the automated analyzer software (MLA–GXMAP and SPL-DZ mode), and the EDS Espirit Bruker microanalysis system (20 Kve).

3.2. Assessment of Potential Recovery/Reuse

In the initial stage, a multivariate statistical analysis utilizing the clustering method was conducted, combining complete linkage and Euclidean distance [37]. Physical-chemical parameters of the samples were employed for this analysis. A dendrogram was generated, which revealed distinct groupings based on specific characteristics and established a potential reuse matrix for these wastes. Four main parameters were identified for the analysis of the observed groups: (1) Evaluation of the main mineralogy and its grouping based on potential reuse; (2) identification of contaminants with a high level of critical risk and contamination; (3) analysis of particles size; and (4) assessment of Au content. This analysis allowed for a more targeted approach in selecting samples for laboratory tests based on their potential for reuse.

Composite samples were then created to represent each group aiming to encompass the maximum variation range for each element with reuse potential. The tables below present the variations observed in the tested samples, ensuring that all values fall within the range identified for each composite group.

3.2.1. Gold Extraction

Various laboratory-scale scenarios were carried out to evaluate the potential recovery of Au [34,38], considering the specific characteristics of each structure. Therefore, three different setups were conducted, involving grinding, leaching, calcination, and, in the case of CDS2, flotation (refer to Figure S1). In addition, these setups were designed to be easily adaptable and applicable to metallurgical plants in the region should a viable and efficient reuse scenario arise.

In the first scenario, samples were ground to a particle size of 74 µm, with 80% of the particles falling within this range, after a liberation-by-size analysis for sulfides and gold particles. The calcination step was disregarded, and the samples were directly subjected to leaching. For Au extraction, bottle roll tests were performed using a leaching solution containing 2000 mg/kg of cyanide (NaCN) and 4000 mg/kg of lime (CaO), with a solid-to-liquid ratio of 50%.

In the second test, specifically designed for the waste characteristics in the CDS2 area, the sample underwent grinding to the particle size of 74 µm using a ball mill, followed by pre-concentration via flotation. This flotation step involved two phases (rougher and cleaner), with the addition of 150 mg/kg of $CuSO_4$ for particle activation, 30 mg/kg of collectors (xanthate and Sodium Diphosphate—INT214), and 60 mg/kg of mibcol foaming agent. The latter was also added during the milling step. The resulting concentrate was calcined in a muffle at 700 °C to facilitate access to the gold included in the sulfide particles and subsequently leached in a bottle with a solid-to-liquid ratio of 50%, using a leaching solution containing 2000 mg/kg of NaCN and 4000 mg/kg of CaO. The rougher and cleaner tailings were combined and subjected to leaching under the same conditions as the concentrate.

The third setup involved grinding the material to a particle size of 74 µm using ball mills, followed by calcination in a muffle at 700 °C. For Au extraction, the calcinated material was placed in bottles containing a solution with 40% solids, comprising 2000 mg/kg of NaCN and 6000 mg/kg of CaO. The extraction process occurred over 24 h, divided into two stages with a pre-airing period of 2 h. The residues from this stage will be submitted to tests for recovery of As and Sb and new products.

3.2.2. Recovery and Stabilization of Arsenic and Antimony

A protocol based on the methodology described by [12] was employed for samples with potential Sb extraction due to defined similarities in characteristics. The objective of the test was to recover Sb and As thermally by volatilizing and collecting them downstream as oxide by-products. Waste samples underwent two tests in a quartz rotary and horizontal klin, with a final temperature of 850 °C, lasting for 6 h, and with a gas mixture of 20% CO and 80% N_2 (Procedure 4). The second test (Procedure 5) was conducted in two phases,

reaching a final temperature of 930 °C, and lasting for 16 h, with 3% O_2 and 97% N_2 (Figure S2a).

Regarding the sample with potential As stabilization and reuse, the protocol outlined in the DST-s GlassLock™ patent process [11] was followed. This process involved mixing the tailing samples with silica, hematite, and sodium carbonate, followed by subjecting them to an oven at temperatures ranging from 1000 °C to 1200 °C and atmospheric pressure for two hours. This treatment resulted in a glass product containing stable forms of oxides, including As and Sb (Procedure 6—Figure S2b).

3.2.3. Recovery of Gangue Minerals

The utilization of triboelectrostatic separation has demonstrated promising results in producing by-products from Au tailings [39]. Additionally, selective grinding and pneumatic concentration techniques are also considered favorable for this type of material, as they are dry-cleaning processes with minimal environmental impacts [40]. The objective of selective grinding and pneumatic separation is to pulverize minerals with a hardness of less than five on the Mohs scale and separate the fraction smaller than 8 μm for concentration. Thus, these methods enable the generation of multiple products from a single source [41–43].

Therefore, after prioritizing samples, the chosen method for assessing the potential generation of alternative products involved: (1) grinding in a pendular mill with hot gas at 450 °C; (2) pneumatic separation into three granulometric fractions (fine, less than 8 μm; intermediate, 30–8 μm; and coarse, greater than 30 μm); and (3) triboelectrostatic concentration of the fine fraction (Figure S3).

Consequently, three potential products were generated and analyzed to investigate their potential use in civil industries and as fertilizer, among other applications.

4. Results and Discussion

4.1. Main Properties of Tailing Materials

4.1.1. Chemical Composition

Table 1 provides a summary of the chemical results for potential valuable elements in each structure. Au is present in all the characterized samples, with the highest concentrations observed in CA samples and the lowest in the MV Group. Anomalous values for other elements are also observed when comparing the sample groups. This detailed information is crucial for subsequent stages, such as the study of reuse potential and the assessment of the environmental impacts associated with waste disposal [34]. The major and trace elements are presented in Tables S1 and S2.

4.1.2. Grain Size Distribution

Granulometric distribution is a crucial parameter for determining the reuse potential and appropriate destination for these materials. As they have already undergone previous grinding and size reduction stages, their particle size distribution presents challenges and complexities for reuse studies [44,45].

Figure 3 illustrates the particle size distribution (PSD) of the samples. In general, 80% of the particles fall within the range of 2–63 μm, classifying them as silty. The samples from the CDS2 structure are coarser, while CA samples contain a higher proportion of clay particles.

Table 1. Statistical summary of potential value elements for the structures' tailings samples.

Structure	N [1]	Element	Mean	SD [2]	Min [3]	Max [4]	N [1]	Element	Mean	SD [2]	Min [3]	Max [4]	N [1]	Element	Mean	SD [2]	Min [3]	Max [4]
BIC	162	Ag (mg/Kg)	0.441	0.211	0.07	0.79	162	Au (mg/Kg)	0.59	1.17	0.025	7.26	111	Cr (mg/kg)	337	156	144	628
CDS1	175		1.54	0.449	1.5	7	175		0.363	0.235	0.025	2.17	150		283	58.1	166	490
CDS2	293		1.52	0.237	1.5	4	293		0.742	0.937	0.24	12.7	293		198	38.8	118	323
CO	282		1.51	0.134	1.5	3	282		0.911	0.715	0.003	8.71	282		142	50.3	40	423
MV	615		0.515	1.66	0.25	13.8	615		0.126	0.353	0.001	5.17	615		137	126	13.3	650
ISO	266		1.37	0.42	0.05	1.5	266		0.649	0.793	0.001	5.99	251		102	79.3	0.1	311
CA	230		8.49	2.29	0.05	15	230		2.39	1.08	0.001	9.45	230		98.3	36.9	0.1	308
BIC	111	Mo (mg/kg)	0.914	0.351	0.49	1.85	111	As (%)	0.179	0.338	0.001	2.18	70	Pb (mg/kg)	163	148	7	429
CDS1	150		1.68	0.733	1.5	7	150		0.122	0.403	0.001	5.00	150		51.6	18.1	4	100
CDS2	291		1.5	0.0	1.5	1.5	291		0.093	0.095	0.001	0.657	111		69.6	28.2	16	171
CO	282		2.12	2.55	1.5	23	282		0.223	6.01	0.001	58.8	248		46	22.4	4	124
MV	321		2.17	3.06	0.5	11.6	321		0.595	5.97	0.001	87.5	293		30.9	71.9	2.03	564
ISO	266		1.37	0.42	0.05	1.5	266		0.717	0.945	0.001	5.7	133		30	89.1	0.1	749
CA	230		7.2	1.78	0.05	10	230		0.725	0.466	0.001	4.80	218		241	64.4	0.1	383
BIC	162	Co (mg/kg)	54.5	35	19.3	137	162	Sb (%)	0	0	0	0.002	111	Cu (%)	0.005	0.009	0.001	0.06
CDS1	175		93.4	39.2	18	273	175		0.013	0.01	0.001	0.056	150		0.007	0.001	0.001	0.012
CDS2	293		21.4	6.22	4	42	293		0.104	0.184	0.001	0.988	293		0.01	0.008	0.001	0.04
CO	282		19.6	11.7	4	76	282		0.003	0	0.003	0.003	282		0.019	0.018	0.001	0.266
MV	615		34.6	46.2	5.53	361	615		0.001	0	0.001	0.001	615		0.001	0	0.001	0.001
ISO	266		33.1	34.1	0.10	214	266		0.002	0	0.002	0.002	251		0.04	0.046	0.001	0.17
CA	230		132	35.8	0.10	195	230		0.004	0.008	0.001	0.059	230		0.086	0.029	0.001	0.16
BIC	163	Cd (mg/kg)	0.148	0.056	0.03	0.24												
CDS1	51.6		1.5	0	1.5	1.5												
CDS2	69.6		1.5	0	1.5	1.5												
CO	46		1.52	0.277	1.5	5												
MV	30.9		0.285	0.259	0.05	0.95												
ISO	30		1.34	0.461	0.05	1.5												
CA	241		1	0.866	0.05	1.5												

[1] N = number of samples; [2] SD = standard deviation; [3] Min—minimum; and [4] Max—maximum.

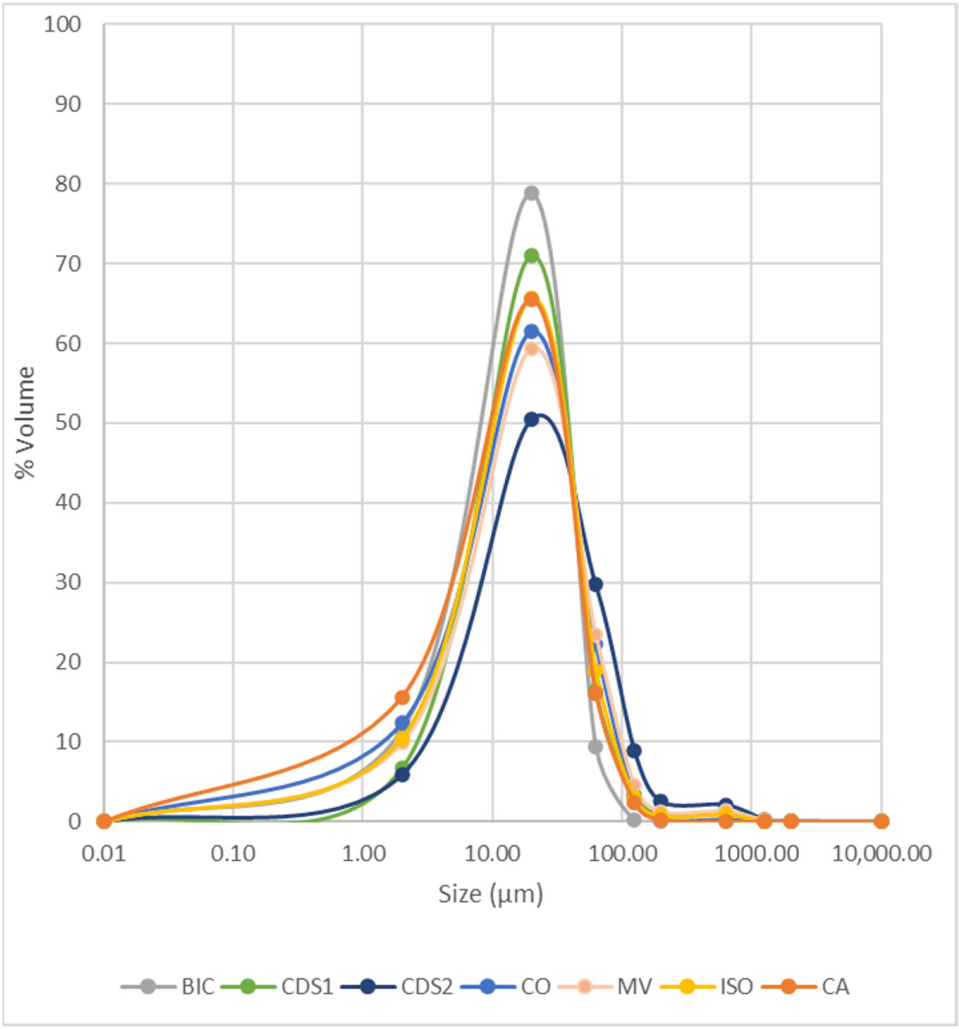

Figure 3. Particle size distribution of waste samples.

This information is valuable for guiding and designing reuse tests, such as civil construction aggregates, which requires larger particle sizes. Typically, products within the sand fraction, e.g., [45], are discarded at this stage of characterization. However, alternative possibilities will be explored, considering other characterization parameters outlined in Section 4.2.

4.1.3. Mineralogical Composition

Tables 2 and S3 present the mineralogy of Au tailing samples from the IQ.

With the exception of CA samples, the quartz content in the tailings is generally greater than 30%, with CO samples having the highest levels (>50%). Silicates belonging to the Muscovite Group are also present, particularly in samples from the ISO, CDS1, and MV structures. Additionally, well-preserved carbonates such as Ankerite and Siderite were identified in CO and BIC samples.

Relic sulfides are observed in all structures, indicating the potential for acid mine drainage. Therefore, the recovery and reuse of metals from these sulfides can also serve as an environmentally sound alternative [13,46]. The main sources of S, particularly in CO, ISO, and BIC structures, are Pyrite, Arsenopyrite, and Pyrrhotite. In CDS2, the presence of Berthierite also contributes to the presence of Sb.

Table 2. Mineralogy of Au tailing samples from the IQ. Analyses are a result of the combination of SEM, optical microscopy, and XRD.

Mineral	Chemical Composition (Ideal Formula)	BIC (Wt%)	CDS1 (Wt%)	CDS2 (Wt%)	CO (Wt%)	MV (Wt%)	ISO (Wt%)	CA (Wt%)
Quartz	SiO_2	31.57	34.18	35.6	55.8	37.83	36.65	15.6
Feldspar Group								
Albite	$NaAlSi_3O_8$	5.33	0.07	1.11	0.37	7.56	2.81	1.5
Anorthite	$CaAl_2Si_2O_8$	-	0.07	0.053	0.01	0.03	0.01	0.053
K feldspar	$KAlSi_3O_8$	0.12	1.18	1.27	0.39	0.73	1.22	-
Phyllosilicates								
Biotite	$KMg_{2.5}Fe_{2+0.5}AlSi_3O_{10}(OH)_{1.75}F_{0.25}$	0.11	1.74	1.26	0.16	2.55	0.52	1
Muscovite	$KAl_3Si_3O_{10}(OH)_{1.9}F_{0.1}$	6.53	38.46	29	5.69	28.85	20.58	12.8
Chlorite	$(Mg,Fe)_3(Si,Al)_4O10(OH)_2 \cdot (Mg,Fe)_3(OH)_6$	2.44	3.34	5.01	6.12	1.28	5.83	3.3
Oxides								
Hematite	Fe_2O_3	-	17.09	0.378	8.86	9.06	8.95	56.8
Fe antimoniate	FeSb(As)O	-	0.07	0.806	-	-	-	-
Rutile/Anathase	TiO_2	0.19	0.29	0.599	0.49	0.60	0.56	0.599
Carbonates								
Ankerite	$Ca(Fe, Mg, Mn)(CO_3)O_2$	16.84	0.02	9	11.2	1.49	0.85	1
Siderite	$FeCO_3$	2.92	0.17	7.2	7.25	0.01	8.94	-
Calcite	$CaCO_3$	0.02	0.05	5.4	2.25	0.23	-	0.2
Sulfates								
Jarosite (Sb)	$KFe(SO_4)_2(OH)_6$ and $(H_3O)Fe(SO_4)2(OH)_6$	-	-	1.00	-	-	-	-
Gypsum	$CaSO_4\ 2H_2O$	-	-	2.00	0.03	-	-	7.00
Sulfides	Total	9.92	0.03	0.36	1.61	0.23	6.85	0.17
Pyrite	$Fe^{2+}S_2$	5.31	0.03	0.08	0.5	0.06	0.22	0.002
Pyrrhotite	$Fe^{2+0.95}S$	2.06	-	0.041	0.79	0.148	4.7	0.004
Arsenopyrite	$Fe^{3+}AsS$	2.52	-	0.056	0.24	0.022	1.71	0.056
Berthierite	$FeSb_2S_4$	-	-	0.141	-	-	-	-
Chalcopyrite	$CuFeS_2$	0.01	-	0.028	-	-	0.21	-
Gesdorffite	NiAsS	0.02	-	-	-	-	-	0.01
Covellite	CuS	-	-	-	0.07	-	0.01	0.1
Sphalerite	ZnS	-	-	0.009	0.01	-	-	-
Au Minerals *								
Au Content (mg/kg)		0.59	0.363	0.742	0.911	0.126	0.649	2.39
Native Au	Au > 80%, Ag, Cu, Hg, Fe, Ni	45	20	158	364	2	60	526
Electrum	Au = 80%, Ag = 20%	8	5	6	10	1	5	42

* Au number particles.

XRD and SEM analyses reveal that Hematite is the main mineral composition of CA and CDS1 samples. This occurrence is attributed to both metallurgical processes and natural oxidation, as the material fed into the CDS1 metallurgical treatment plant consists of oxidized Au ores (Figure 2a).

Sulfates such as Gypsum were also in CA and CDS2 samples, mainly due to treatment steps where lime was used for pH neutralization. Another noteworthy finding in CDS2 samples is the presence of Jarosite, which contains Sb and serves as an indicator of sulfides oxidation, including Berthierite, during the pressure oxidation step (Figure 4b).

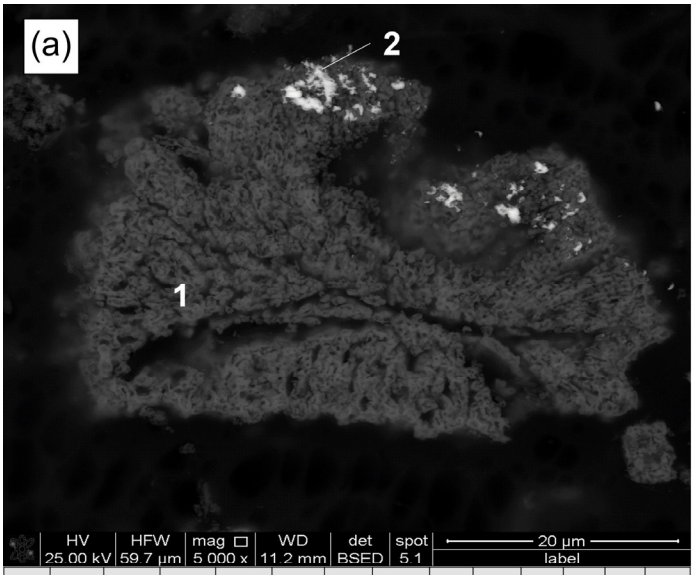

Phase	As (%)	Ag (%)	Pb (%)	Au (%)	Cr (%)	Cu (%)	Fe (%)	O(%)	S(%)	Si (%)	Zn(%)	Ni(%)	Hg (%)
1	1.39		0.101		0.020	0.20	66.16	26.43	4.42	0.32	0.51		
2		1.15		91.16		2.60	2.10				0.96	1.28	1.62

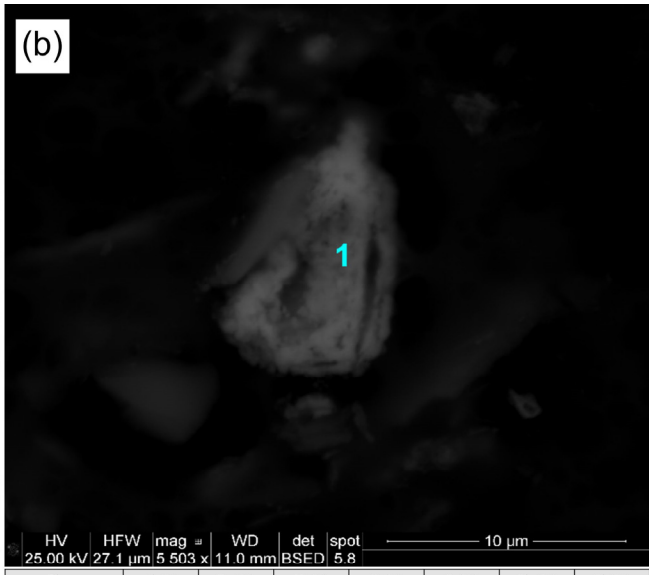

Phase	Al (%)	Fe (%)	K (%)	O (%)	S (%)	Sb (%)	Si (%)
1	7.75	32.89	3.50	36.81	12.07	2.77	1.09

Figure 4. Electronic microscopy images of two phases of CA samples. (**a**) Hematite with As, Pb, S, Cu, and Zn, and (**b**) Jarosite with Sb.

The geochemical study indicates that CA samples have higher concentrations of metals and metalloids, such as As, Cu, Pb, Zn, and Fe. Table 2 shows the dominance of Hematite, but SEM-EDS analysis suggests that these elements were somehow adsorbed in Hematite itself during the metallurgical oxidation process (Figure 4a). S is also present in Hematite, and Fe oxides with As concentration above 40% were rarely detected by EDS.

For this study, the distribution of main minerals according to sample grain size was also assessed. If there is a predominance of a mineral carrying an element of interest for reuse or decontamination within a specific preferred granulometric range, it can guide selective separations or pre-merger possibilities [40,47–50].

Table 3 presents the key mineralogical differences between particle sizes above and below 6 µm.

Table 3. Mineralogy (in two size fractions) by tailing structures. Mineral abbreviations after [51].

Sample	Size Fraction	Mass (%)	Minerals (wt%) *																
			Py	Fe hox/ox	Po	Apy	Qz	Ank	Cal	Ab	Sd	Ms Group	Chl Group	Kfs	Rt	Gp	Ap	Jrs (Sb)	Fe Ant
BIC	>6 µm	88.5	0.001	-	11.2	5.30	66.4	-	-	5.90	0.0	-	7.50	2.57	1.18	-	-	-	-
	<6 µm	15.0	5.94	-	-	-	0.023	2.45	-	0.012	25.8	59.3	6.53	-	-	-	-	-	-
CDS1	>6 µm	93.3	0.013	21.5	0.033	0.013	43.0	0.023	0.063	0.089	0.213	25.8	7.33	1.48	0.360	-	-	-	0.078
	<6 µm	6.67	0.027	8.77	1.25	0.019	25.5	0.016	0.068	0.164	0.750	50.4	0.387	2.72	0.973	-	-	-	8.97
CDS2	>6 µm	94	0.094	-	0.183	0.128	81.4	-	-	2.53	-	10.2	-	2.83	1.32	-	0.459	0.432	0.432
	<6 µm	6	-	-	-	-	0.274	18.8	-	0.013	15.0	51.1	10.4	0.080	0.050	4.17	0	0.061	0.049
CO	>6 µm	87.6	-	-	0.822	0.402	93.1	-	-	0.613	-	0.602	2.68	0.637	0.805	-	0.335	-	-
	<6 µm	12.4	2.69	-	0.031	-	0.695	38.2	-	0.014	24.7	18.2	15.4	0.033	0.032	-	-	-	-
MV	>6 µm	90.1	0.170	10.3	0.063	0.025	43.4	1.70	-	8.64	0.013	32.8	1.47	0.787	0.680	-	-	-	-
	>6 µm	90.1	0.170	10.3	0.063	0.025	43.4	1.70	-	8.64	0.013	32.8	1.47	0.787	0.680	-	-	-	-
ISO	>6 µm	89.5	0.00	16.5	-	3.20	68.7	-	-	5.19	0.0	-	3.20	2.27	1.03	-	-	-	-
	<6 µm	10.5	11.8	0.488	0.552	0.016	0.295	2.13	-	0.121	22.5	51.7	10.4	0.034	0.036	-	-	-	-
CA	>6 µm	84.4	-	76.1	-	-	20.4	-	-	1.78	-	0.905	-	-	0.768	-	-	-	-
	<6 µm	15.0	-	8.37	-	-	3.59	3.68	0.736	0.833	-	44.7	12.1	-	0.180	25.8	-	-	-

* Py = Pyrite; Fe hox/ox = Fe Hydroxide/Oxide; Po = Pyrrhotite; Apy = Arsenopyrite; Qz = Quartz; Ank = Ankerite; Cal = Calcite; Ab = Albite; Sd = Siderite; Ms = Muscovite; Chl = Chlorite; Kfs = K-Feldspar; Rt = Rutile; Gp = Gypsum; Ap = Apatite; Jrs = Jarosite; and Fe ant = Fe Antimoniate.

In support of the reuse tests, the main observations were as follows:

- There is a predominance of 24 common minerals among the structures, with Quartz, Iron Oxides, Muscovite, Ankerite, Chlorite, Siderite, and Albite being the main ones;
- Depending on the structure, Quartz is commonly found in fractions above 6 µm and can be a potential product for applications in, e.g., civil construction. Previous research [52] suggests that tailings should have a SiO_2 concentration above 15% and a maximum size of less than 1 mm to be used as an aggregate. The inclusion of tailings as fine aggregate in concrete has been shown to increase compressive strength. It is generally recommended to substitute no more than 30% of the fine aggregates with tailings to maintain durability. Additionally, the solidification of metals within the tailings can be beneficial, and the clinker can be produced using the tailings;
- Minerals from the Muscovite and Chlorite Groups are the most commonly found in fractions below 6 µm and can be utilized in products such as fertilizers and rock meal. Research [52] identified important specifications for these types of products, including the presence of Ca and Mg as carbonates, high alkalinity, good availability of P, average availability of K, and the presence of micronutrients such as Zn, B, Cu, Fe, and Mn;
- The distribution of sulfides, if present, varies depending on each structure. Generally, they are found in finer fractions at BIC, CDS1, MV, and ISO, while coarser fractions contain sulfides in other structures. These sulfides may indicate the presence of noble metals such as Au, particularly because they are derived from this metal treatment process;
- CDS2 samples contain minerals and Sb compounds in finer fractions;
- CA samples are rich in Fe Oxides in fractions coarser than 6 µm.
- Consequently, this analysis allows for the identification of different potential products that can be derived from a single source.

In addition to the previously described potentials identified through granulometry and mineralogy, it is noteworthy that Au particles are present in all samples from different structures. SEM analysis reveals that Au is present in its native form, with low associations of Fe, Ni, Pb, and Hg, as well as in the form of an electrum. In the CO, BIC, ISO, and CDS2 structures, Au is associated and enclosed within sulfides (Figures 5a–d and S4) alongside Quartz. Furthermore, in the CDS2 sample, Au is also observed in association with Jarosite (Figure 5d). In the MV and CDS1 structures (Figures 5e,f and S4), fine Au particles are found to be associated with Quartz and Muscovite, while in the CA structure, the main association is identified as fine Au particles within Hematite pores (Figures 5g and S4).

4.2. Tests for Potential Recovery/Reuse

Physical-chemical data, including mineralogy, chemistry, and PSD, from each tailing structure were used for multivariate analysis to cluster observations. The objective was to assess similarities among characteristics and determine the potential for grouping to facilitate and guide the reuse tests.

The dendrogram (Figure 6) reveals the presence of five groups, as CDS2, CA, and ISO samples exhibit distinctive characteristics with similarities to the remaining samples below 66%. The key variables influencing these groupings were the concentrations of Au, S, Sb, Fe, As, and types of sulfides. Table S4 provides the parameter values obtained from the centroid of each group, thus showcasing their unique identities.

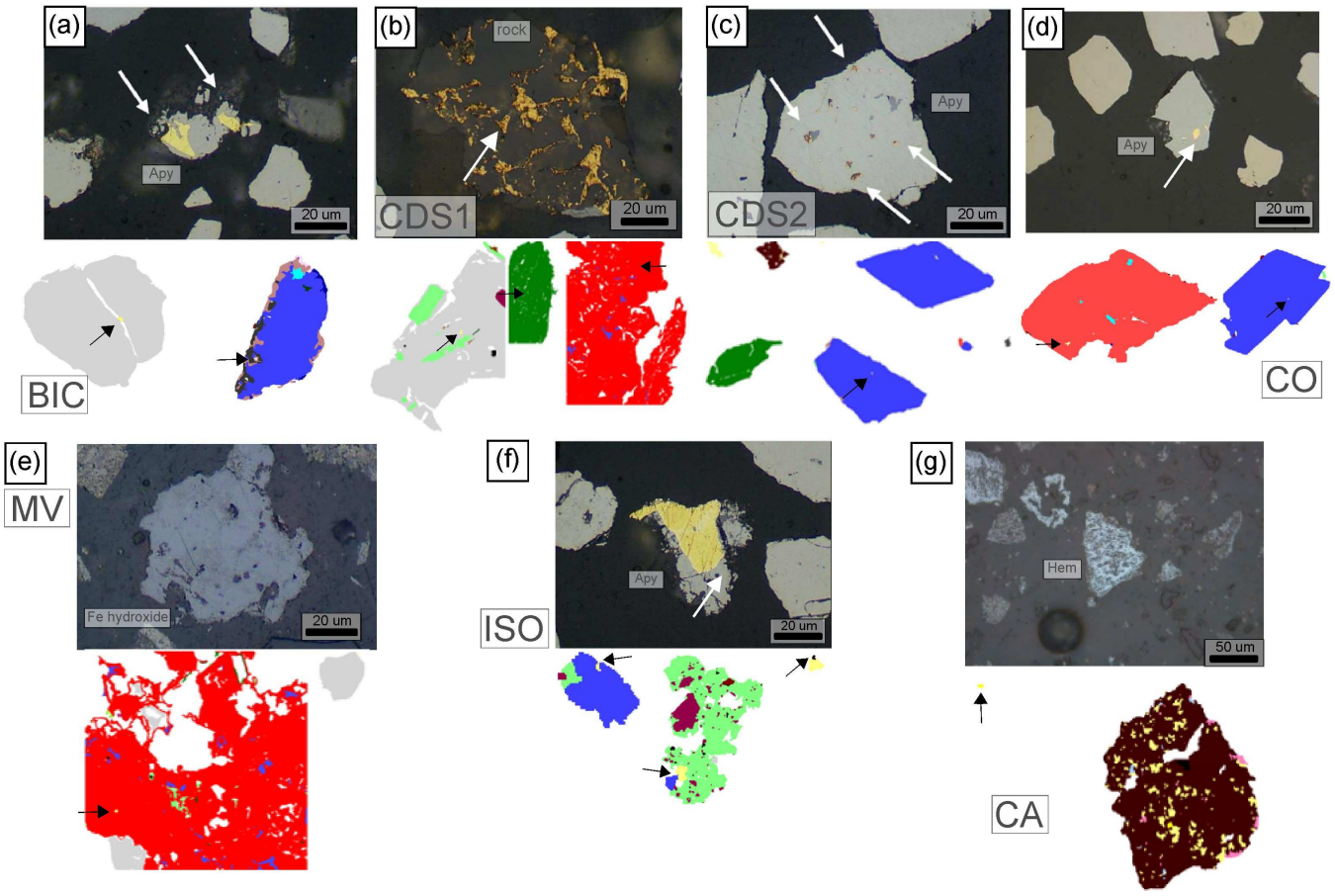

Figure 5. False color electron images and microphotographs (reflected light and parallel Nicols) illustrate the presence of Au-bearing particles (indicated by yellow and black/white arrows) and Fe Hydroxide. Mineral abbreviations follow [51]. (**a**) BIC—enclosed Au particles in Quartz (gray) and Arsenopyrite. (**b**) CDS1—Au particles enclosed in rock minerals (Quartz and Muscovite) and Fe Hydroxide. (**c**) CDS2—Free Au particles and Muscovite (dark green) along with Arsenopyrite. (**d**) CO—Au particles enclosed in Pyrite (orange) and Arsenopyrite (blue). (**e**) MV—fine Au particles enclosed in Fe Hydroxide (red). (**f**) ISO—Au particles enclosed in Arsenopyrite and rock minerals (Chlorite—light green). (**g**) CA—free Au particles and Au particles within porous Hematite (brown).

Based on this multivariate analysis, a matrix was constructed to identify the potential for reuse (Table 4). The matrix is divided into three categories: high (H), medium (M), and low (L), determined by the composition and occurrence modes of elements such as Sb, Fe, As, and, of course, Au.

Considering the relevant potential of Au across all Groups, an assessment was conducted to evaluate its overall recovery potential. For the recovery tests targeting Sb, samples from Group 2 (CDS2) were used, with additional attempts to recover As. To explore the utilization of Fe and potentially generate other products, samples representing Group 5 were selected. Lastly, to determine the potential for generating alternative products (as indicated in Table 4), samples representing Groups 1 and 4 were chosen.

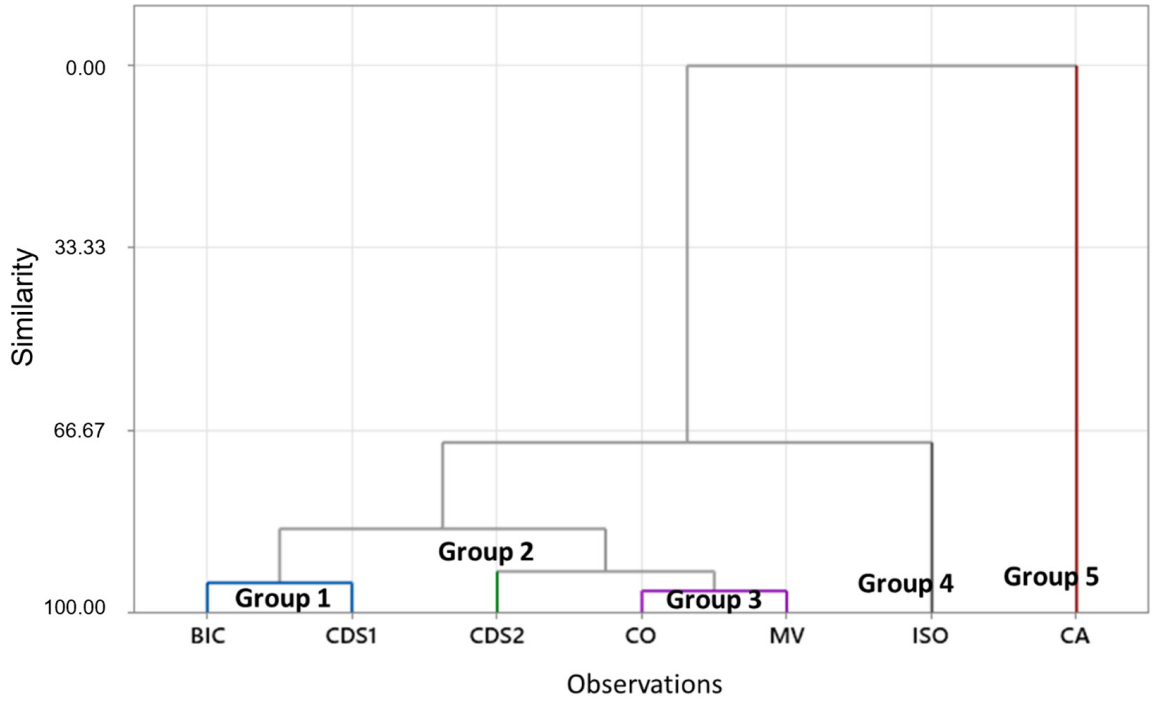

Figure 6. Dendrogram (generated using complete linkage and Euclidean distance), which illustrates the grouping of tailings samples for the purpose of guiding reuse tests. Group 1: BIC and CDS1 samples. Group 3: CO and MV samples. The remaining groups (2, 4, and 5) did not exhibit sufficient similarity within the 100% to 70% range and therefore were not grouped.

Table 4. Potential recovery of metals, metalloids, and other products based on chemical, textural, and mineralogical characteristics.

Group	Samples	Au Recovery	As Recovery	Sb Recovery	Fe Recovery	Others *
Group 1	BIC + CDS1	H	L	L	L	H
Group 2	CDS2	H	M	H	L	H
Group 3	CO + MV	H	L	L	L	H
Group 4	ISO	H	H	L	M	H
Group 5	CA	H	H	L	H	L

* K and Si enrichment.

4.2.1. Au Recovery

Table 5 presents the recovery results obtained from the tests conducted in three different scenarios for each Group. Samples from Group 5 were exclusively tested using Procedures 1 and 3, as they did not exhibit characteristics that warranted concentration through the flotation stage.

The aggressiveness of the procedures increases from Procedure 1 to Procedure 3. In the roasting step, the aim was to open up the sulfide minerals to gain access to the encapsulated gold.

The obtained results demonstrate a promising potential for Au recovery. Procedure 1 yields better recoveries for Group 3 due to the presence of Au grains attached to sulfides and Quartz (Table 5 and Figure S4). Procedure 2 was more suitable for Group 2 as it contains both sulfide and oxidized sources of Au. In the oxidized samples, Au is attached, while in the sulfide samples, it is enclosed. Therefore, concentrating the sulfides and subjecting them to calcination is crucial for achieving higher recovery rates. However, for the other groups, there are losses in flotation recovery due to sulfide losses during the flotation stage and their limited oxidation. Procedure 3 results in higher recoveries for Groups 1 and 4

because calcination provides access to locked gold in sulfides, in addition to the pre-existing Au oxide.

Table 5. Summary of metallurgical test results for Au reuse in each group of tailing samples. Modified from [38].

Group	Structures	Calculated Feed Grade (mg/kg)	Au Mineralogical Association	Procedure 1 *1	Procedure 2 *2	Procedure 3 *3
				(% Au Recovery)		
1	BIC + CDS1 *4	0.740	sulfides and Quartz	29.5	30.9	77.7
2	CDS2	0.742		49.9	70.7	34.9
3	CO + MV *4	0.735		71.8	59.4	66.4
4	ISO	1.16		64.0	48.2	78.5
5	CA	2.39	Fe Oxides	32.2	-	0.60

*1 Leach in 74 µm, *2 Flotation + Calcine + Leach in 74 µm, *3 Calcine + Leach in 74 µm, *4 CDS1 and MV presented the amount of gold particles in oxide, as well.

Despite having the highest Au content among all procedures, samples from Group 5 exhibit poor recoveries. This can be attributed to the presence of very fine Au inclusions associated with Hematite (Figure 4a). This association poses a challenge for the treatment and reuse of Au in this cluster.

In general, Table 5 highlights that good levels of recovery are achieved through the same procedures for Groups 1 and 4. This information is significant as it would facilitate the industrial re-treatment of these structures with minimal investment, considering their proximity to metallurgical units that already have the necessary stages in Au production [13,33]. Although the calcination step is not covered, samples from Groups 2 and 3 can also be considered in this potential reuse setup. However, for Group 5, further viability studies are required, as additional stages and technological advancements are necessary.

The residues from this stage will be submitted to tests for recovery of As and Sb and new products. The next items, the residues produced in this item, will be submitted to the recovery of As and Sb (4.2.2) and total reuse (4.2.3).

4.2.2. Arsenic and Antimony Recovery

For the assessment of Sb and As recovery potential in composite samples, Groups 2 and 5 were selected (Table 4). In the case of Group 2, the same procedure described by [12] was employed due to the presence of Sb and As in sulfides and sulfates. For samples in Group 5, the vitrification procedure was followed, mainly due to the high Fe content required for this type of test. The results are summarized in Table 6.

Table 6. Summary of metallurgical test results for Sb and As recovery for Groups 2 and 5.

Group	Samples	Sb Feed Grade (%)	As Feed Grade (%)	Procedure 4 (One Stage of Klin Roasting)		Procedure 4 (Two Stages of Klin Roasting)		Procedure 5 (As e Sb Vitrification)	
				Sb Recovery (%)	As Recovery (%)	Sb Recovery (%)	As Recovery (%)	Sb Recovery (%)	As Recovery (%)
2	CDS2	0.104	0.010	2.00	1.00	18.7	3.97		
5	CA	0.080	0.776					75.0	93.7

In the tested scenario for Group 2, a low recovery is achieved, consistent with the observations made by [12]. The best setup would involve two stages of calcination, which would result in higher volatilization rates and, consequently, better recovery.

On the other hand, the tests conducted for Group 5 successfully recovered these elements. Most of them are neutralized in the form of glass (Figure 7), making them potential inputs for various applications such as civil construction.

Figure 7. Glass formed from GlassRock^{TM} methodology demonstrates the possibility of As and Sb recovery and its use as an industrial product.

These tests provide an opportunity for exploring new paths, not only for the reuse of Group 5 but also for other structures and operational facilities facing challenges in the treatment of waste containing hazardous metals and metalloids such as As and Sb.

4.2.3. Selective Grinding, Pneumatic and Triboelectrostatic Separation—Other Products and Opportunities

For the tests aimed at identifying the potential for generating other products, samples were chosen based on their mineralogical size distribution. Two Groups were chosen: Group 3, which exhibited similarities with Groups 1, 2, and 4, and Group 5, which was the most distinct. The objective of these tests was to assess the possibility of pre-concentration and evaluate the potential for generating multiple products from the same source.

In this stage, the samples underwent selective grinding and pneumatic separation, resulting in two products from each feed: a fine fraction below 6 µm and a coarse fraction above 30 µm (Groups 3 and 5—Figure S5). The intermediate product is further subjected to triboelectrostatic separation, resulting in the generation of two additional products. Table 7 provides an overview of the mass distribution and the chemical quality of these products.

Table 7. Summary of size separation results of Groups 4 and 5.

Group	Samples	Size (µm)	S1 *	S2 **		Products Chemical Quality									
			w (%)	w (%)		Al (%)	As (%)	Au (mg/kg)	Ca (%)	Fe (%)	K (%)	Mg (%)	Na (%)	S (%)	Si (%)
3	CO + MV	>30	69.8	-	-	3.04	0.036	0.690	3.68	6.95	0.856	1.44	0.190	1.13	30.4
		30–6	23.1	E1	14.6	26.2	0.100	0.260	2.10	9.30	4.00	1.0	0.400	0.900	44.4
				E2	8.56	6.50	0.400	1.19	8.00	17.9	1.00	2.10	0.700	4.10	44.4
		<6	7.04	-	-	11.4	0.100	0.890	1.97	9.88	3.70	1.62	0.264	1.73	20.6
5	CA	>30	71.5	-	-	1.19	0.062	3.16	0.339	53.0	0.307	0.436	0.107	0.063	7.99
		30–6	21.9	E1	7.67	8.50	2.00	1.36	3.40	49.3	1.70	1.70	0.800	0.30	24.8
				E2	14.3	6.50	2.00	2.46	3.40	58.4	0.900	1.00	0.500	0.40	19.8
		<6	6.62	-	-	3.64	0.169	1.13	0.286	47.5	0.763	1.43	0.175	0.073	8.41

* S1: Selective grinding and pneumatic separation and ** S2: triboeletrostatic separation.

The results presented in Table 7 indicate that there are similar mass distributions in terms of granulometric separations for both Groups. However, chemical enrichment of certain elements is observed in fractions of Group 3. The triboeletrostatic separation process proves to be relatively efficient in concentrating Al and K (probably Muscovite) for fertilizer production (63%), as well as sulfides, Fe, Au, and As (37%). Nevertheless, when evaluating

other size fractions (>30 μm and <6 μm), it can be observed that the previous steps are not as effective as expected.

Regarding Group 5, the triboelectrostatic separation process does not yield satisfactory results. However, enrichment of Fe and Au in coarse fractions (>30 μm) and relative depletion of Si can be observed. However, there are also limitations in achieving good separation rates in the preceding steps.

These observations can be explained by the mineralogical complexity of the samples, which compromised the efficiency of the tests. Further reassessment and identification of improvements are needed, as some elements show enrichment in specific fractions. However, in these initial tests, no generation of by-products from a single source has yet been identified. This does not invalidate the potential of these samples but rather highlights the challenges involved in transforming them into multiple products solely through physical separations. For the use of this technique and the production of new products, further studies are needed.

5. Conclusions

This study explores various possibilities to add value to different Au mining tailings in the Iron Quadrangle region. The waste materials were characterized and distinguished for concentration tests targeting different elements, with Au being the most promising element for recovery. Calcination, leaching, and flotation techniques showed promise for recovering Au, particularly in samples from the CDS mine. The results obtained from these techniques were comparable to successful Au mines in Brazil and South Africa.

On the other hand, the tests demonstrated that toxic elements such as Sb and As could be effectively reused in the form of glass, thereby adding value and offering a solution for the disposal of hazardous waste. Although the generation of other products using dry cleaning techniques was not highly effective, it showed promise due to the enrichment of elements such as Au, Fe, Al, and K in specific fractions.

The information obtained from this study can be further optimized, and economic analyzes need to be conducted for each value-adding technique. Future research should explore different methods and equipment to identify further opportunities for improvement and value addition through modifications or additional setups.

Supplementary Materials: The following supporting information can be downloaded at: https://www.mdpi.com/article/10.3390/min13070863/s1, Figure S1: Au extraction potential in (a) Calcination + Leaching, (b) Direct Leaching and (c) Flotation + Calcination + Leaching, modified from [34]; Figure S2: Sb and As extraction potential in (a) rotative klin and (b) GlassLock^{TM}, modified from [11,35]; Figure S3: Test flowchart for generation of three potential input-generating products in the civil, fertilizer and other industries; Figure S4: Gold deportment chart by structure complementing Figure 5 of this study; Figure S5: Image of tested samples in the selective grinding test, pneumatic and triboelectrostatic separation from (a) Group 4 and (b) Group 5; Table S1: Statistical summary of major elements for the structures' tailings samples; Table S2: Statistical summary of trace elements for the structures' tailings samples; Table S3: Mineralogical composition by XRD of <2 mm fraction. Mineral abbreviations after [51]; Table S4: Parameters of each group's centroids, which defined grouping by observations.

Author Contributions: Conceptualization, M.G.L., T.M.V., A.P.M.R., R.M.F.F., F.G., J.G.d.M.F. and M.F.M.; methodology, M.G.L., T.M.V., A.P.M.R., R.M.F.F., F.G., J.G.d.M.F. and M.F.M.; software, M.G.L. and I.D.D.; validation, M.G.L., T.M.V., A.P.M.R., R.M.F.F., F.G., J.G.d.M.F., M.F.M. and I.D.D.; formal analysis, M.G.L., T.M.V., A.P.M.R., R.M.F.F., F.G., J.G.d.M.F., M.F.M. and I.D.D.; investigation, M.G.L., T.M.V., A.P.M.R., R.M.F.F., F.G., J.G.d.M.F., M.F.M. and I.D.D.; resources, M.G.L., T.M.V., A.P.M.R., R.M.F.F., F.G., J.G.d.M.F. and M.F.M.; data curation, M.G.L., T.M.V., A.P.M.R. and R.M.F.F.; writing—original draft preparation, M.G.L.; writing—review and editing, M.G.L., T.M.V., A.P.M.R., R.M.F.F. and G.R.D.; visualization, M.G.L., T.M.V., A.P.M.R., R.M.F.F. and G.R.D.; supervision, M.G.L., T.M.V., A.P.M.R. and R.M.F.F.; project administration, M.G.L., T.M.V., A.P.M.R., R.M.F.F., F.G., J.G.d.M.F. and M.F.M.; funding acquisition, M.G.L., T.M.V., A.P.M.R., R.M.F.F., F.G., J.G.d.M.F. and M.F.M. All authors have read and agreed to the published version of the manuscript.

Funding: This research was funded by Fundação para a Ciência and Tecnologia (FCT) through projects UIDB/04683/2020, UIDP/04683/2020, and Nano-MINENV 029259 (PTDC/CTA-AMB/29259/2017).

Data Availability Statement: The data presented in this study are available upon request from the corresponding author. The data are not publicly available due to high amounts of data.

Acknowledgments: We thank our colleagues from the Instituto de Ciências da Terra (ICT), the Microscopy Center from Universidade Federal de Minas Gerais (CM-UFMG), and from AngloGold Ashanti, who provided insights and expertise that greatly assisted this research; Fundação para a Ciência and Tecnologia (FCT) for financial aid; and MSc Alexandre Orlandi and Jean Philippe Mai for laboratory support and reuse tests of other elements such as As, Sb, Fe, and K. The authors are deeply grateful for the support of all expert reviewers.

Conflicts of Interest: The authors declare no conflict of interest.

References

1. Gomes, A.C.F. Estudo de Aproveitamento de Rejeito de Mineração. Master's Thesis, Universidade Federal de Minas Gerais, Belo Horizonte, Brazil, February 2017.
2. Gorakhki, M.H.; Bareither, C.A. Sustainable reuse of mine tailings and waste rock as water-balance covers. *Minerals* **2017**, *7*, 128. [CrossRef]
3. Circular Economy of Metals and Responsible Mining. Available online: https://blogs.egu.eu/network/gfgd/2018/04/24/circular-economy-of-metals-and-responsible-mining/ (accessed on 1 April 2023).
4. Mineração no Brasil Colonial. Available online: https://brasilescola.uol.com.br/historiab/mineracao-no-brasil-colonial.htm (accessed on 10 April 2023).
5. Jones, H.; Boger, D.V. Sustainability and waste management in the resource industries. *Ind. Eng. Chem. Res.* **2012**, *51*, 10057–10065. [CrossRef]
6. Silva, A.P.M.; Viana, J.P.; Cavalcante, A.L.B. *Diagnóstico dos Resíduos Sólidos da Atividade de Mineração de Substâncias Não Energéticas*; Instituto de Pesquisa Econômica Aplicada: Brasília, Brazil, 2012; 46p.
7. Shafiee, S.; Topal, E. An overview of global gold market and gold price forecasting. *Resour. Policy* **2010**, *35*, 178–189. [CrossRef]
8. Moraes, S.L.; Motta, F.G.; Massola, C.P.; Saccoccio, E.M.; Júnior, M.C. Rejeitos de mineração: Um olhar do cenário brasileiro-Parte I: Cadeia produtiva. In *Anais dos Seminários de Redução, Minério de Ferro e Aglomeração, Proceedings of the 18° Simpósio de Mineração, São Paulo, Brasil, 2–6 Editora Blucher Octomber 2017*; Institute for Technological Research: São Paulo, Brazil, 2017. [CrossRef]
9. ANM. Available online: https://www.gov.br/anm/pt-br (accessed on 12 April 2023).
10. Mesquita, P.P.D.; Carvalho, P.S.L.; Ogando, L.D. Desenvolvimento e inovação em mineração e metais. *BNDES Set.* **2021**, *43*, 325–361.
11. Lalancette, J.M.; Lemieux, D.; Nasrallah, K.; Curiel, G.G.; Barbaroux, R. Method for Vitrification of Arsenic And Antimony. U.S. Patent 9981295 B2, 29 May 2015. Available online: https://patents.google.com/patent/US9981295B2/en (accessed on 1 January 2020).
12. Lemos, M.G.; Valente, T.M.F.; Marinho Reis, A.P.; Fonsceca, R.; Dumont, J.M.; Ferreira, G.M.M.; Delbem, I.D. Geoenvironmental study of gold mining tailings in a circular economy context: Santa Barbara, Minas Gerais, Brazil. *Mine Water Environ.* **2021**, *40*, 257–269. [CrossRef]
13. Lemos, M.; Valente, T.; Marinho Reis, P.; Fonseca, R.; Delbem, I.; Ventura, J.; Magalhães, M. Mineralogical and geochemical characterization of gold mining tailings and their potential to generate acid mine drainage (Minas Gerais, Brazil). *Minerals* **2021**, *11*, 39. [CrossRef]
14. Parviainen, A.; Soto, F.; Caraballo, M.A. Revalorization of Haveri Au-Cu mine tailings (SW Finland) for potential reprocessing. *J. Geochem. Explor.* **2020**, *218*, 106614. [CrossRef]
15. Study on the Critical Raw Materials for the EU 2023—Final Report. Available online: https://single-market-economy.ec.europa.eu/publications/study-critical-raw-materials-eu-2023-final-report_en (accessed on 14 June 2023).
16. European Commission. *Communication from the Commission to the European Parliament, the Council, the European Economic and Social Committee and the Committee of the Regions: Critical Raw Materials Resilience: Charting a Path Towards Greater Security and Sustainability, 474 Final*; European Commission: Brussels, Belgium, 2020; 28p.
17. Antunes, M.; Fernandes, R.; Pinheiro, A.; Valente, T.M.F.; Nascimento, S. Potential of reuse and environmental behavior of ochre-precipitates from passive mine treatment. In *IMWA 2010 Proceedings, Proceedings of the International Mine Water Association Symposium—Mine Water and Innovative Thinking, Sydney, Canada, 5–9 September 2010*; Wolkersdorfer, C., Freund, A., Eds.; Wolkersdorfer & Freund: Aachen, Germany; pp. 205–208.
18. Nwaila, G.T.; Ghorbani, Y.; Zhang, S.E.; Frimmel, H.E.; Tolmay, L.C.; Rose, D.H.; Nwaila, P.C.; Bourdeau, J.E. Valorisation of mine waste-Part I: Characteristics of, and sampling methodology for, consolidated mineralised tailings by using Witwatersrand gold mines (South Africa) as an example. *J. Environ. Manag.* **2021**, *295*, 113013. [CrossRef]
19. Sibanda, L.K.; Broadhurst, J.L. Exploring an alternative approach to mine waste management in the South African gold sector of the article. In Proceedings of the 11th ICARD | IMWA | MWD Conference–"Risk to Opportunity", Pretoria, South Africa, 10–14 September 2018; Wolkersdorfer, C., Sartz, L., Weber, A., Burgess, J., Tremblay, G., Eds.; pp. 1130–1135.

20. Dehghani, A.; Ostad-Rahimi, M.; Mojtahedzadeh, S.H.; Gharibi, K.K. Recovery of gold from the Mouteh Gold Mine tailings dam. *J. South. Afr. Inst. Min. Metall.* **2009**, *109*, 417–421.
21. Cairncross, K.H.; Tadie, M. Life cycle assessment as a design consideration for process development for value recovery from gold mine tailings. *Miner. Eng.* **2022**, *183*, 107588. [CrossRef]
22. Muir, A.; Mitchell, J.; Flatman, S.R.; Sabbagha, C. A practical guide to re-treatment of gold processing residues. *Miner. Eng.* **2005**, *18*, 811–824. [CrossRef]
23. PanAfrican Resources Mineral Resources and Mineral Reserves Report for the Year Ended 30 June 2018. Available online: https://www.miningnewsfeed.com/reports/annual/Pan-African-Resources-MRMR-report-2018.pdf (accessed on 12 April 2023).
24. Monte, M.B.M.; Grisol, S.; Duque, T.F.M.B.; Fenelon, P.A.; Junior, G.G.O. Flotação seletiva para o reprocessamento de rejeitos provenientes do processo de lixiviação da Kinross Paracatu. *Braz. Appl. Sci. Rev.* **2020**, *4*, 2720–2728. [CrossRef]
25. Ince, C. Reusing gold-mine tailings in cement mortars: Mechanical properties and socio-economic developments for the Lefke-Xeros area of Cyprus. *J. Clean. Prod.* **2019**, *238*, 117871. [CrossRef]
26. Mapinduzi, R.P.; Bujulu, P.; Mwegoha, W.J. Potential for reuse of gold mine tailings as secondary construction materials and Phytoremediation. *Int. J. Environ. Sci.* **2016**, *7*, 49–61. [CrossRef]
27. Yao, G.; Liu, Q.; Wang, J.; Wu, P.; Lyu, X. Effect of mechanical grinding on pozzolanic activity and hydration properties of siliceous gold ore tailings. *J. Clean. Prod.* **2019**, *217*, 12–21. [CrossRef]
28. Sánchez-Peña, N.E.; Narváez-Semanate, J.L.; Pabón-Patiño, D.; Fernández-Mera, J.E.; Oliveira, M.L.S.; Boit, K.; Tutikian, B.F.; Crissien, T.J.; Pinto, D.C.; Serrano, I.D.; et al. Chemical and nano-mineralogical study for determining potential uses of legal Colombian gold mine sludge: Experimental evidence. *Chemosphere* **2018**, *191*, 1048–1055. [CrossRef]
29. Swaroop, G.; Bulbule, K.A.; Parthasarathy, P.; Shivakumar, Y.; Muniswamy, R.; Annamati, R.; Priyanka, D. Application of Gold Ore Tailings (GOT) as a source of micronutrients for the growth of plants. *Int. J. Sci. World* **2013**, *1*, 68–78.
30. Goldfarb, R.J.; Groves, D.I.; Gardoll, S. Orogenic gold and geologic time: A global synthesis. *Ore Geol. Rev.* **2001**, *18*, 1–75. [CrossRef]
31. Lobato, L.M.; Ribeiro-Rodrigues, L.C.; Vieira, F.W.R. Brazil's premier gold province. Part II: Geology and genesis of gold deposits in the Archean Rio das Velhas greenstone belt, Quadrilátero Ferrífero. *Miner. Depos.* **2001**, *36*, 249–277. [CrossRef]
32. Roeser, H.M.P.; Roeser, P.A. O Quadrilátero Ferrífero-MG, Brasil: Aspectos sobre sua história, seus recursos minerais e problemas ambientais relacionados. *Geonomos* **2010**, *18*, 33–37. [CrossRef]
33. Moura, W. Especiação de Cianeto para Redução do Consumo no Circuito de Lixiviação de Calcinado da Usina do Queiróz. Master's Thesis, Universidade Federal de Minas Gerais, Belo Horizonte, Brazil, 2005.
34. Lemos, M.; Valente, T.; Reis, P.; Fonseca, R.; Pantaleão, J.P.; Guabiroba, F.; Filho, J.G.; Magalhães, M.; Delbem, I. Caracterização Mineralógica, Geoquímica e Potencial de Valorização de Resíduos de Mineração de Ouro (Minas Gerais, Brasil). In Proceedings of the XXIX Encontro Nacional de Tratamento de Minérios e Metalurgia Extrativa, Armação dos Búzios, Brazil, 25–28 September 2022.
35. Ashanti, A.G. *AngloGold Ashanti AngloGold Ashanti Recommendations*; AngloGold Ashanti: Johannesburg, South Africa, 2016.
36. Valente, T.M.; Antunes, M.; Sequeira Braga, A.; Prudêncio, M.I.; Marques, R.; Pamplona, J. Mineralogical attenuation for metallic remediation in a passive system for mine water treatment. *Environ. Earth Sci.* **2012**, *66*, 39–54. [CrossRef]
37. Hastie, T.; Tibshirani, R.; Friedman, J. *The Elements of Statistical Learning: Data Mining, Inference, and Prediction*, 2nd ed.; Springer: New York, NY, USA, 2009; 764p.
38. Lemos, M.; Valente, T.; Reis, P.M.; Fonseca, R.; Pantaleão, J.P.; Guabiroba, F.; Filho, J.G.; Magalhães, M.; Afonseca, B.; Silva, A.R.; et al. Geochemistry and mineralogy of auriferous tailings deposits and their potential for reuse in Nova Lima Region, Brazil. *Sci. Rep.* **2023**, *13*, 4339. [CrossRef]
39. Cho, H.C.; Oh, W.; Han, O.H.; Kang, H.H.; Lee, J.S. Recovery of valuable materials from gold mine tailings. In *Separation Technologies for Minerals, Coal, and Earth Resources*, 7th ed.; Young, C.A., Luttrell, G.H., Eds.; Society for Mining, Metallurgy, and Exploration: Englewood, NJ, USA, 2012; pp. 277–287.
40. Ferguson, D.N. A basic triboelectric series for heavy minerals from inductive electrostatic separation behaviour. *J. South. Afr. Inst. Min. Metall.* **2010**, *110*, 75–78.
41. Jordan, C.E.; Sullivan, G.V.; Davis, B. *Report of Investigations 8457, Pneumatic concentration of Mica*; US Bureau of Mines Report Investigations: Pittsburgh, PA, USA, 1980; pp. 1–24.
42. Emrullahoglu, O.F.; Kara, M.; Tolun, R.; Celik, M.S. Beneficiation of calcined colemanite tailings. *Powder Technol.* **1993**, *77*, 215–217. [CrossRef]
43. Yang, J.; Xu, W.; Deng, X.; Li, H.; Ma, S. Research on the Selective Grinding of Zn and Sn in Cassiterite Polymetallic Sulfide Ore. *Minerals* **2022**, *12*, 245. [CrossRef]
44. Peiravi, M.; Dehghani, F.; Ackah, L.; Baharlouei, A.; Godbold, J.; Liu, J.; Mohanty, M.; Ghosh, T. A review of rare-earth elements extraction with emphasis on non-conventional sources: Coal and coal byproducts, iron ore tailings, apatite, and phosphate byproducts. *Min. Metall. Explor.* **2021**, *38*, 1–26. [CrossRef]
45. Okereafor, U.; Makhatha, M.; Mekuto, L.; Mavumengwana, V. Gold mine tailings: A potential source of silica sand for glass making. *Minerals* **2020**, *10*, 448. [CrossRef]

46. Valente, T.; Grande, J.A.; De La Torre, M.L. Extracting value resources from acid mine drainages and mine wastes in the Iberian Pyrite Belt. In Proceedings of the IMWA 2016—Mining Meets Water—Conflicts and Solutions, Leipzig, Germany, 11–15 July 2016; Drebenstedt, C., Paul, M., Eds.; Technische Universität Bergakademie: Freiberg, Germany, 2016; pp. 1339–1340.
47. Luckeneder, S.; Giljum, S.; Schaffartzik, A.; Maus, V.; Tost, M. Surge in global metal mining threatens vulnerable ecosystems. *Glob. Environ. Chang.* **2021**, *69*, 102303. [CrossRef]
48. Marion, C.; Grammatikopoulos, T.; Rudinsky, S.; Langlois, R.; Williams, H.; Chu, P.; Awais, M.; Gauvin, R.; Rowson, N.A.; Waters, K.E. A mineralogical investigation into the pre-concentration of the Nechalacho deposit by gravity separation. *Miner. Eng.* **2018**, *121*, 1–13. [CrossRef]
49. Yang, X.; Wang, H.; Peng, Z.; Hao, J.; Zhang, G.; Xie, W.; He, Y. Triboelectric properties of ilmenite and quartz minerals and investigation of triboelectric separation of ilmenite ore. *Int. J. Min. Sci. Technol.* **2018**, *28*, 223–230. [CrossRef]
50. Bada, S.O.; Tao, D.; Honaker, R.Q.; Falcon, L.M.; Falcon, R.M.S. A study of rotary tribo-electrostatic separation of South African fine coal. *Int. J. Coal Prep. Util.* **2010**, *30*, 154–172. [CrossRef]
51. Whitney, D.L.; Evans, B.W. Abbreviations for names of rock-forming minerals. *Am. Mineral.* **2010**, *95*, 185–187. [CrossRef]
52. Gou, M.; Zhou, L.; Then, N.W.Y. Utilization of tailings in cement and concrete: A review. *Sci. Eng. Compos. Mater.* **2019**, *26*, 449–464. [CrossRef]